A constructive combination of antireflection and intermediate-reflector layers for a–Si / μc–Si thin film solar cells

Chandan Das, Andreas Lambertz, Juergen Huepkes, Wilfried Reetz, and Friedhelm Finger

Citation: Appl. Phys. Lett. **92**, 053509 (2008);
View online: https://doi.org/10.1063/1.2841824
View Table of Contents: http://aip.scitation.org/toc/apl/92/5
Published by the American Institute of Physics

A constructive combination of antireflection and intermediate-reflector layers for *a*-Si/μc-Si thin film solar cells

Chandan Das,[a] Andreas Lambertz, Juergen Huepkes, Wilfried Reetz, and Friedhelm Finger
IEF5-Photovoltaik, Forschungszentrum Juelich GmbH, 52425 Juelich, Germany

(Received 27 November 2007; accepted 21 January 2008; published online 8 February 2008)

This device design approach combines sputter-deposited TiO_2 antireflection layer (ARL) and plasma-enhanced chemical vapor deposition-grown SiO_x intermediate-reflector layer (IRL) in superstrate *a*-Si/μc-Si thin film solar cell. The loss of current from either the component cells with individual application of ARL and IRL has been recovered with their combined application. With both ARL and IRL in *a*-Si/μc-Si cell, (a) the top cell current and (b) the sum of top and bottom cell current increases. An initial efficiency of 11.8% [V_{oc}=1.42 V, FF=0.74, J_{sc} (top)=11.5 mA cm^{-2}, J_{sc} (bottom)=11.2 mA cm^{-2}] is achieved from such an *a*-Si/μc-Si cell with a total Si layer thickness less than 2 μm. © *2008 American Institute of Physics*. [DOI: 10.1063/1.2841824]

In the area of thin film *a*-Si based solar cell technology, one important task is to increase the "stabilized" efficiency of the solar cells. This task includes both the improvement of silicon materials used in the device and the device design itself. The multijunction device structure leads the *a*-Si based thin film solar cells to reach an efficiency of 15% until date.[1,2] To further improve the performance of such a solar cell, one needs to critically review the device design to overcome the inherent losses. In case of a glass superstrate based device structure, an optical loss occurs due to refractive index (n) mismatch between the transparent conducting oxide viz. ZnO ($n\sim1.9$) and Si ($n\sim3.5$) layers. A layer of TiO_2 ($n\sim2.5$) at ZnO and silicon interface has shown to have potential to act as an antireflection layer (ARL) to minimize the optical loss due to refractive index mismatch.[3] Very recently, it has been demonstrated that an increase of short-circuit current density (J_{sc}) is possible from multijunction *a*-Si based solar cells using TiO_2 as a refractive index matching layer.[4] Again by the same time, another approach demonstrated a control over the distribution of currents from the subcells of an *a*-Si/μc-Si cell using a plasma-enhanced chemical vapor deposition (PECVD)-grown SiO_x as intermediate reflector layer (IRL) by introducing a mismatched refractive index ($n\sim2$) at Si/Si ($n\sim3.5$) interface and this IRL could preferentially illuminate the *a*-Si top cell, which is prone to light induced degradation compared to the bottom microcrystalline cell.[5,6] However, both the individual approaches with ARL and IRL result some current loss in either of the component cells in an *a*-Si/μc-Si device structure.[4,6] In the present work, these two approaches with optical layers, namely TiO_2 as ARL and SiO_x as IRL have been constructively combined to gain J_{sc} from an *a*-Si/μc-Si solar cell through precise current management. The performance of the solar cells using ARL and IRL has been demonstrated in this paper. The gain in efficiency combining the optical layers into the standard cell design should entirely contribute to the higher stabilized efficiency of the *a*-Si/μc-Si solar cell, since no modification in the silicon layers has been done for this improvement compared to the standard one.

The deposition of TiO_2 thin films has been done by rf-magnetron sputtering. The identical process chamber and use of similar deposition regime as that of front contact ZnO, add minimum effort in alteration of the deposition system or process control for the inclusion of TiO_2 to the TCO development infrastructure. Again, as the SiO_x films have been developed by PECVD technique, it is quite advantageous regarding system integration to introduce a PECVD-grown Si based IRL deposition step between two silicon layer depositions. Therefore, the ARL and IRL discussed in this article invite almost no alteration in the system and process control over the conventional *a*-Si based thin film solar cell development. In the experimental process, the TiO_2 films have been sputtered from a TiO_2:Nb_2O_5 (99:1) target in 0.2% O_2 in Ar ambient with a power density of 1.5 W cm^{-2} by rf-magnetron system at a chamber pressure of 2 mTorr and deposited at room temperature. The deposition rate of the TiO_2 films is 0.5 Å s^{-1} and a thickness between 50 and 75 nm has been used for device application. In this process, a typical conductivity of the TiO_2 films has been obtained as 1.0×10^{-7} S cm^{-1} from coplanar measurement of the samples deposited on Corning Eagle 2000 glass substrate. The refractive index (n) calculated from photothermal deflection spectroscopy (PDS) measurement is typically around 2.45 at infrared wavelength region. The detailed optimization and characterization of the TiO_2 films have been described elsewhere.[7] The SiO_x thin films have been deposited by rf-PECVD (13.56 MHz) with gas flow ratios SiH_4:H_2=1:200, PH_3:SiH_4=1:50, and SiH_4:CO_2=2:3 with a power density of 0.35 W cm^{-2} at a substrate temperature below 200 °C. The films are intentionally *n*-type doped and the typical conductivity from coplanar measurement on Corning Eagle 2000 glass substrate is around 1.5×10^{-5} S cm^{-1}. The deposition rate is 1.6 Å s^{-1} and, for the device application, a thickness between 75 and 100 nm has been deposited. The refractive index is calculated as $n\sim2.4$ in the infrared wavelength region and the absorption coefficient (α) at 2 eV lies around 1.5×10^5 cm^{-1} from PDS measurement for the SiO_x film. Further information regarding the deposition conditions and the layer properties of SiO_x could be found elsewhere.[5] In the fabrication of *p-i-n* solar cells, the glass substrates are used in superstrate configuration. The standard solar cells

[a]Electronic mail: c.das@fz-juelich.de.

TABLE I. Performance of *a*-Si/μc-Si double junction cells for the standard, with ARL, with IRL, and with both ARL and IRL showing subcell J_{sc} obtained from quantum efficiency measurements.

			J_{sc} (mA cm^{-2})		
	V_{oc} (V)	FF	Top	Bottom	η (%)
Standard	1.41	0.73	11.0	11.4	11.3
ARL	1.42	0.72	10.8	12.2	11.0
IRL	1.42	0.71	11.4	10.7	10.8
ARL and IRL	1.42	0.74	11.5	11.2	11.8

are deposited on ZnO coated glass, where the ZnO is texture-etched with HCl.[8] The solar cells have been fabricated following a device design: glass/ZnO(texture etched)/*a*-Si(*p-i-n*)/μc-Si(*p-i-n*)/ZnO/Ag. The silicon thin films have been deposited by PECVD technique. In case of the solar cells with ARL, the TiO_2 layer has been deposited on the texture-etched ZnO and covered with a very thin film of ZnO (<10 nm) to protect it from H_2 plasma reduction process during the exposure to PECVD silicon deposition.[3] In case of the solar cells with IRL, the SiO_x layer has been deposited at the *n*/*p* junction of two consecutive *p-i-n* subcells. The cells have been measured under 1 sun, AM 1.5 illumination. The quantum efficiency and, thereby, the integrated J_{sc} have been calculated for the top and bottom component cells at short-circuit conditions with AM 1.5 spectrum. The lowest current between that from the two component cells has been considered as the J_{sc} of the solar cells and accounted for the efficiency calculations. The sum of the currents from the top and bottom component cells is considered as the "total current" from the device in some discussions.

In the Table I, performance of the *a*-Si/μc-Si solar cells has been given for the standard one, the one with ARL, the one with IRL, and the one with both ARL and IRL. In case of the cells with optical layers, the layers have been incorporated as additions into the standard cell configuration. In the first step of this device design approach, ARL has been incorporated in the standard cell following the device design: glass/ZnO(texture etched)/TiO_2/ZnO(10 nm)/*a*-Si(*p-i-n*)/μc-Si(*p-i-n*)/ZnO/Ag. The quantum efficiency curves for the component cells are shown in Fig. 1, where the total quantum efficiency as the sum of individual quantum efficiencies of the component cells is also depicted. In case of the cell with ARL, the quantum efficiency of the top cell decreases in the region of wavelength <500 nm and increases slightly in the region >500 nm, which results a drop in J_{sc} of the top cell by 2%. However, the quantum efficiency of the bottom cell increases in the wavelength region from 500 to 1000 nm and results 7% increase in the J_{sc} of the bottom cell compared to the standard one. The total current increases from 22.4 to 23.0 mA cm^{-2}, which is due to the increase of the quantum efficiency in the long wavelength region in spite of the decrease in short wavelength region for the *a*-Si/μc-Si cell.

In the next step, IRL has been incorporated in the device following the design: glass/ZnO(texture etched)/*a*-Si(*p-i-n*)/SiO_x(*n*)/μc-Si(*p-i-n*)/ZnO/Ag and the performance of the *a*-Si/μc-Si solar cell is given in the Table I. The quantum efficiency curves are shown in Fig. 2 for the cell with IRL and compared with the standard one. The quantum efficiency improves for the top cell with introduction of IRL and the most pronounced improvement is in the wavelength region from 550 to 750 nm. The J_{sc} of the top cell increases by 4% in this case compared to the standard one. On the other hand, the quantum efficiency of the bottom cell decreases for the cell with IRL and the J_{sc} of the bottom cell drops by 6% compared to the standard cell. Similar loss of current is also observed in the reports dealing with SiO_x based IRL.[5,6] As a result, with application of the IRL, the total quantum efficiency curve shows a decrease in the longer wavelength and the total current decreases from 22.4 to 22.1 mA cm^{-2} compared to the standard cell.

In the final step, both the ARL and IRL have been incorporated in the device design as follows: glass/ZnO(texture etched)/TiO_2/ZnO(10 nm)/*a*-Si(*p-i-n*)/SiO_x(*n*)/μc-Si(*p-i-n*)/ZnO/Agand the performance of the solar cell is shown in the Table I. The quantum efficiency curves are

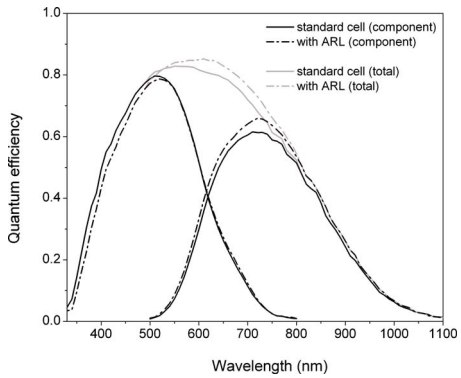

FIG. 1. (Color online) Quantum efficiency curves for the component top and bottom cells (black lines) and total quantum efficiency as the sum of that of the top and bottom cells (gray lines) for the *a*-Si/μc-Si standard cell and the cell with ARL.

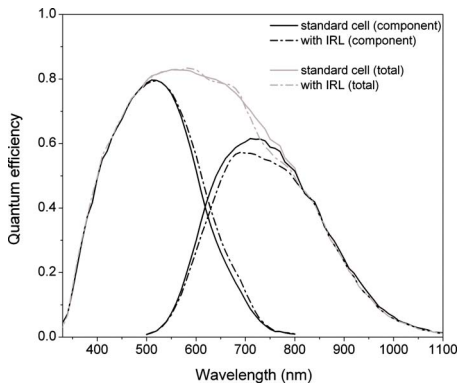

FIG. 2. (Color online) Quantum efficiency curves for the component top and bottom cells (black lines) and total quantum efficiency as the sum of that of the top and bottom cells (gray lines) for the *a*-Si/μc-Si standard cell and the cell with IRL.

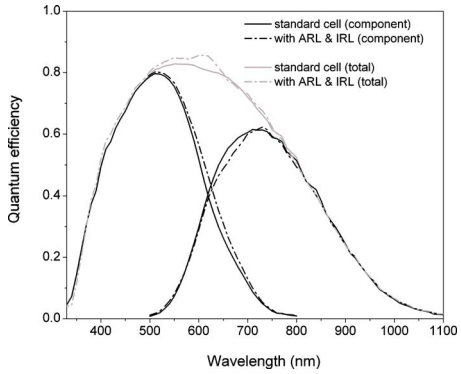

FIG. 3. (Color online) Quantum efficiency curves for the component top and bottom cells (black lines) and total quantum efficiency as the sum of that of the top and bottom cells (gray lines) for the *a*-Si/μc-Si standard cell and the cell with both ARL and IRL.

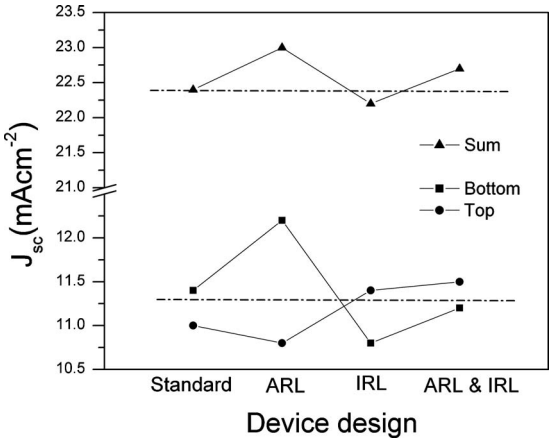

FIG. 4. The short-circuit current density (J_{sc}) of the top cell, bottom cell, and the sum of the J_{sc}s of the top and bottom cells against each device design: standard, with ARL, with IRL and with both ARL and IRL. The lines drawn in the graph are guides to the eyes.

shown in Fig. 3 for the cell with both ARL and IRL and compared with the standard one. The quantum efficiency of the top cell improves over the 500–750 nm wavelength range and results in a 5% increase of the J_{sc} of the top cell. The slight variation in quantum efficiency in the wavelength range of <400 nm could be attributed to the small difference in *p*-layer thickness from one cell to another. The quantum efficiency of the bottom cell decreases to some extent around 700 nm and corresponds to only a 2% drop in the J_{sc} of the bottom cell. Thus, with application of both the ARL and IRL in the device, the J_{sc} of the top cell increases from 11.0 to 11.5 mA cm^{-2} and the drop of J_{sc} of the bottom cell due to sole application of IRL is almost recovered. The total quantum efficiency of the cell shows a net improvement in the wavelength range of 500 –650 nm as shown in Fig. 3 and this results in an increase of total current from 22.4 to 22.7 mA cm^{-2} compared to the standard cell. In the present work, the incorporation of the both ARL and IRL results in an efficiency of 11.8% with a J_{sc} limited by that of the bottom cell, compared to the standard cell of efficiency 11.3% with a J_{sc} limited by that of the top cell. To visualize the effect of applications of the ARL and IRL, the J_{sc} of the subcells and the sum of the J_{sc}s of the subcells have been plotted in Fig. 4 against each device design. In Fig. 4, it is exhibited that even starting from an already optimized *a*-Si/μc-Si cell with a high J_{sc} of 11 mA cm^{-2}, further improvement of J_{sc} is possible with application and proper combination of antireflection and intermediate-reflector layers. Thus, with both the ARL and IRL in the device, the improvement of J_{sc} of the top cell, maintaining almost the same J_{sc} from the bottom cell, enables one to either reduce the *a*-Si active layer thickness of the top cell or to increase the active μc-Si layer thickness of the bottom cell for further improvement of the stability of the *a*-Si/μc-Si solar cell.

In conclusion, the TiO_2 as ARL and SiO_x as IRL have been developed by sputtering and PECVD processes, respectively, and incorporated into the superstrate *a*-Si/μc-Si solar cell design. The combined application of the optical layers has been demonstrated to improve the current from the top *a*-Si cell and to minimize the loss of current from bottom μc-Si cell so that the sum of the top and bottom cell current increases too. Thus, with application of antireflection and intermediate-reflector layers as a constructive combination, an efficiency of 11.8% has been achieved from an *a*-Si/μc-Si solar cell with total Si layer thickness less than 2 μm.

This work has been done under the European Union project ATHLET (Contract No. 019670). The authors would like to thank T. Melle, A. Doumit, R. van Aubel, and J. Klomfass for their assistance in the experiments and H. Wang and A. Gordijn for some measurement and discussion.

[1] S. Fukuda, K. Yamamoto, A. Nakajima, M. Yoshimi, T. Sawada, T. Suezaki, M. Ichikawa, Y. Koi, M. Goto, T. Meguro, T. Matsuda, T. Sasaki, and Y. Tawada, *Proceedings of the 21st European Photovoltaic Solar Energy Conference*, Dresden, Germany (WIP, Munich, 2006), pp. 1535–1538.
[2] B. Yan, G. Yue, J. M. Owens, J. Yang, and S. Guha, *Proceedings of the 4th World Conference on Photovoltaic Energy Conversion*, Hawaii, USA (IEEE, New York, 2006), pp. 1477–1480.
[3] T. Fujibayashi, T. Matsui, and M. Kondo, Appl. Phys. Lett. **88**, 183508 (2006).
[4] C. Das, M. Berginski, J. Huepkes, A. Gordijn, J. Kirchhoff, W. Reetz, A. Lambertz, F. Finger, and W. Beyer, *Proceedings of the 22nd European Photovoltaic Solar Energy Conference*, Milan, Italy (WIP, Munich, 2007), pp. 2112–2114.
[5] A. Lambertz, A. Dasgupta, W. Reetz, A. Gordijn, R. Carius, and F. Finger, *Proceedings of the 22nd European Photovoltaic Solar Energy Conference*, Milan, Italy (WIP, Munich, 2007), pp. 1839–1842.
[6] P. Buehlmann, J. Bailat, D. Domine, A. Billet, F. Feltrin, and C. Ballif, Appl. Phys. Lett. **91**, 143505 (2007).
[7] M. Berginski, C. Das, A. Doumit, J. Huepkes, B. Rech, and M. Wuttig, *Proceedings of the 22nd European Photovoltaic Solar Energy Conference*, Milan, Italy (WIP, Munich, 2007), pp. 2079–2082.
[8] O. Kluth, G. Schoepe, J. Huepkes, C. Agashe, J. Mueller, and B. Rech, Thin Solid Films **442**, 80 (2003).